Turkish Journal of Electrical Engineering & Computer Sciences

http://journals.tubitak.gov.tr/elektrik/

Research Article

Turk J Elec Eng & Comp Sci
(2018) 26: 2088 – 2103

doi:10.3906/elk-1708-281

Real-time implementation of three-level inverter-based D-STATCOM using neuro-fuzzy controller

Resul ÇÖTELİ[1], **Hakan AÇIKGÖZ**[2,*], **Beşir DANDIL**[3], **Servet TUNCER**[4]

[1]Department of Energy Systems Engineering, Faculty of Technology, Fırat University, Elazığ, Turkey
[2]Department of Electrical Science, Vocational High School, Kilis 7 Aralık University, Kilis, Turkey
[3]Department of Mechatronics Engineering, Faculty of Technology, Fırat University, Elazığ, Turkey
[4]Department of Electrical and Electronics Engineering, Faculty of Technology, Fırat University, Elazığ, Turkey

Received: 25.08.2017 • **Accepted/Published Online:** 03.04.2019 • **Final Version:** 27.07.2018

Abstract: A distribution static compensator (D-STATCOM) is a custom power device connected in parallel to a power system to address electric power quality problems caused by reactive power and harmonics. To obtain high performance from a D-STATCOM, the D-STATCOM's dq-axis currents must be controlled in an internal control loop. However, control of the D-STATCOM's currents is difficult because of its nonlinear structure, cross-coupling effect between the d- and q-axis, undefined dynamics, and fast changing load. Therefore, the controller to be preferred for a D-STATCOM should have a nonlinear and robust structure. In this study, a neuro-fuzzy controller (NFC), which is a robust and nonlinear controller, is proposed for dq-axis current control of a D-STATCOM. A DSP-based experimental setup is built for real-time control. The basic building block of the experimental setup is a three-level cascaded inverter. This inverter is constructed by using three IPM intelligent modules. A DS1103 controller card is used for real-time control of the D-STATCOM's experimental setup. The control algorithm is prepared in MATLAB/Simulink software and loaded to the DS1103 controller card. The performance of the NFC current-controlled D-STATCOM is tested for different load conditions: no load to full inductive, no load to full capacitive, full inductive to full capacitive, and full capacitive to full inductive. For this aim, the reactive current setpoint is changed as a step. The experimental results are presented to show the efficiency of the proposed controller under different load conditions.

Key words: D-STATCOM, electric power quality, neuro-fuzzy controller, three-level H-bridge inverter

1. Introduction

The widespread use of power electronic-based equipment and nonlinear and inductive loads have brought power quality problems in distribution systems. The adverse effects of power quality problems are well known. Conventional compensators such as fixed capacitor and reactor banks and static VAR compensators have been widely used for improvement of electric power quality. With the advancement of microprocessor and semiconductor technology, inverter-based custom power devices have been introduced in distribution systems. A distribution static compensator (D-STATCOM) is an inverter-based custom power device and meets the load current compensation requirements such as reactive power compensation, load balancing, and harmonic elimination, as well as voltage regulation under balanced and unbalanced loads [1–4].

The control algorithm is the most important part of a D-STATCOM used for dynamic control of

*Correspondence: hakanacikgoz@kilis.edu.tr

reactive power. The best compensation effect can be obtained by control of the D-STATCOM properly [2, 5]. Conventionally, control of a D-STATCOM is realized by proportional integral (PI) controller(s) designed by means of linear control methods. There are many studies in the literature on PI controller design for D-STATCOM control. In [6], a PI controller was designed by linearizing equations of a phase angle-controlled STATCOM at a specific operating point and neglecting the mathematical model of the inverter. In another work, an AC and DC side mathematical model of a three-phase AC-DC voltage source converter (VSC) was derived and *dq*-axis current and DC voltage control were carried out with a PI controller designed by eliminating cross-coupling terms [7]. The parameters of the digital PI controller were tuned using the mathematical model of the D-STATCOM in [8] and a PI controller design for a D-STATCOM was given in [9]. In [10], a controller design procedure was given for a cascaded-multilevel converter-based STATCOM. In addition, linear quadratic regulator (LQR) and pole placement approaches were proposed in [11]. In these studies, the controller was designed with some assumptions and some neglected points. Therefore, the best possible performance from a D-STATCOM might not be able to be obtained from designed controllers for different operating points.

As an alternative to linear control methods, nonlinear and adaptive control methods have been proposed to improve the dynamic compensation performance of D-STATCOMs. Feedback linearization was used to design a nonlinear controller for STATCOM in [12, 13]. Nonlinear passivity-based approaches were proposed in [14, 15], while an H_∞ control approach was proposed in [16]. Another study covering nonlinear controller design based on differential algebra for a STATCOM was also presented in [17]. A sliding-mode controller was proposed in [18, 19]. In such nonlinear control methods, an exact mathematical model and accurate system parameters are required. Unfortunately, the mathematical model of the D-STATCOM could not be exactly obtained because a D-STATCOM is a system that has a semidefined structure and parameter variations. The design of these controllers is complex. The controller parameters can be updated by using adaptive control methods in real time [20]. When designing the controller for industrial processes by means of above-mentioned control methods, a dynamic model of the system to be controlled is needed. Sometimes, the model of a system may not be possible in practice. There are some processes for which the parameters may be changed from time to time. Recently, systems having semidefined and nonlinear structures and variation of parameters have been controlled by intelligent controllers such as fuzzy logic controllers (FLCs) or artificial neural networks (ANNs) [21]. In the literature, ANN-based control algorithms in [22–24] and FLC-based control algorithms in [25–27] were proposed. It is well known that there are some difficulties in the design of both controllers. There is no standard method for determining the rule base, span, and shape of the memberships in the design of FLCs, whereas the number of hidden layers as well as the number of hidden neurons are determined by trial and error in the design of ANN controllers [28].

A neuro-fuzzy controller (NFC) is a combination of an FLC and ANN, where the FLC functions are performed by the ANN. Problems encountered in the design of ANNs and FLCs could be eliminated by using NFC structures. In addition, the NFC does not need a mathematical model of the system to be controlled. Several studies on NFC control of STATCOMs/D-STATCOMs have been presented in the literature. In [29], an NFC was designed for external control of a STATCOM to improve damping of the rotor speed deviations of its neighboring generators in a 12-bus benchmark power system and obtained simulation results were given. In [30], an NFC was also used for external control of a STATCOM. Although there are a few simulation studies related to external control of STATCOMs based on NFCs, there are no experimental or simulation studies on internal control of D-STATCOMs based on NFCs.

In this paper, the *dq*-axis current of a D-STATCOM is controlled by a nonlinear control strategy-based

NFC. The proposed NFC has singleton rules, two inputs, one output, and four layers. The dq-axis current is controlled by two independent NFC controllers. Inputs of the NFC used in the d-axis are chosen as d-axis current error and change in this error, whereas inputs of the other NFC are q-axis current error and change in q-axis current error. In addition, the outputs of controllers are integrated to improve the tracking capability of the NFC in steady state. To verify the dynamic performance of the NFC current-controlled D-STATCOM, an experimental setup based on a three-level H-bridge inverter is built. dSPACE's DS1103 controller card is used for processing of sensed currents and voltages by Hall effect sensors in the control algorithm and also for generating the gate signals for the inverter. Gate signals for the three-level cascaded inverter are generated with multilevel sinusoidal pulse width modulation (SPWM) technique. When the D-STATCOM is used for load compensation or voltage regulation tasks, it provides reactive current to the point of common coupling (PCC). Therefore, both tasks could be accomplished by using a step change in the reactive current setpoint. Dynamic performance of the NFC current-controlled D-STATCOM is evaluated for reactive current setpoint changing. From experimental results, the NFC current-controlled D-STATCOM shows successful dynamic performance for a step change in reference reactive current (transient and steady-state conditions) with sudden load or voltage variations.

2. Three-level H-bridge inverter-based D-STATCOM

A D-STATCOM is an inverter-based custom power device. It consists of an inverter, DC-link capacitor, coupling transformer/inductance, and control algorithm. The inverter is a basic building block of all converter-based custom power devices. There are two inverter topologies depending on the DC-link source: the voltage source inverter (VSI) and current source inverter (CSI). VSIs convert DC input voltage into AC voltage and CSIs convert DC current into AC current. A common problem in CSIs is related to their higher losses compared with VSIs [31]. In addition, VSIs are a good option for use in industrial applications because of their features such as unity power factor, sinusoidal input current, high performance of the DC voltage, bidirectional power flow, and low harmonic distortion.

A simple VSI produces a square voltage waveform when it switches the DC voltage on and off. It must produce a near sinusoidal AC voltage with minimal waveform distortion [32]. To obtain a fast response from the D-STATCOM, the inverter must be operated at high switching frequency. Total harmonic distortion of inverter output voltage can also be decreased depending on switching frequency. Therefore, PWM inverters are more suitable for D-STATCOM applications [33]. However, there are some limitations in operating at high switching frequency of two-level PWM inverters such as switching losses and constraints of the device rating itself [34]. Depending on the inverter structure and compensation requirements, the semiconductor switches on the inverter can be controlled by various techniques [35].

Recently, multilevel inverters with advantages such as direct connection to the distribution system and improvement of the harmonic content of output voltage compared with conventional two-level PWM inverters operating in the same switching frequency have been used in D-STATCOM applications. Cascaded multilevel inverters among multilevel inverter topologies are the most popular topology because of using the smallest number of components and the flexibility of the circuit layout. Cascaded inverter topology is based on the series connection of H-bridges with separate DC sources. In this inverter structure, the number of output voltage levels can be easily increased by adding or decreased by removing the H-bridges [36]. Today, three-level H-bridge inverters can be connected to distribution systems without using step-down transformers because of commercially available IGBTs with high voltage and current ratings. Therefore, the inverter can be connected

to the grid via coupling inductance. The structure of the three-level H-bridge inverter-based D-STATCOM is shown in Figure 1. As shown in Figure 1, H-bridges are connected to the power grid by means of a coupling inductance at the PCC and one H-bridge unit is used for each phase. DC voltages for these H-bridges are provided by DC-link capacitors.

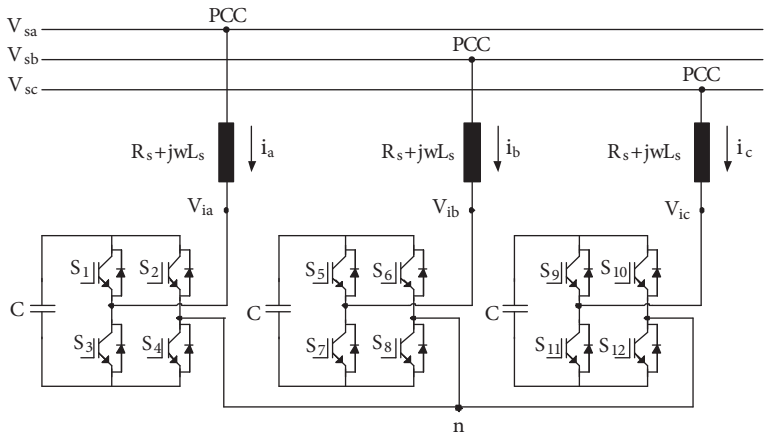

Figure 1. The circuit of the three-level H-bridge inverter-based D-STATCOM.

The basic operation principle of the D-STATCOM is based on two shunt-connected AC sources (grid and D-STATCOM) with the same frequency by means of coupling inductance [37]. Exchange of reactive power between the grid and D-STATCOM is achieved by adjusting the amplitude of the inverter output voltage V_i. If the amplitude of inverter output voltage is greater than grid voltage V_s, the D-STATCOM generates capacitive reactive power. Otherwise, the D-STATCOM absorbs inductive reactive power. If the amplitude of inverter output voltage is equal to grid voltage, the exchange of reactive power between the D-STATCOM and the grid will be zero. Reactive power generated/absorbed by the D-STATCOM is given by the following equation:

$$Q = \frac{V_s}{X}(V_s - V_i \cos\delta). \tag{1}$$

Here, Q is reactive power generated/absorbed by the D-STATCOM, X is the reactance of coupling inductance, and δ is the phase angle between the fundamental voltage of the D-STATCOM and the grid. In D-STATCOM operation, DC-link voltages are held by DC-link capacitors. Since there is no energy source connected to the DC-link, net active power transacted by the D-STATCOM must be zero. In practice, energy losses occur in capacitors and inverter switches. If these losses are not supplied from the grid, the capacitors will discharge. To prevent discharging of capacitors, some active power must be drawn from the grid. Active power absorbed by the D-STATCOM is calculated as follows:

$$P = \frac{V_s \times V_i}{X} \sin\delta. \tag{2}$$

Here, P is active power generated/absorbed by D-STATCOM. From Figure 1, the circuit equation of the

AC side of the H-bridge inverter-based D-STATCOM in *abc* coordinates can be written as follows:

$$\frac{d}{dt}\begin{bmatrix} i_a \\ i_b \\ i_c \end{bmatrix} = \begin{bmatrix} \frac{-R_s}{L_s} & 0 & 0 \\ 0 & \frac{-R_s}{L_s} & 0 \\ 0 & 0 & \frac{-R_s}{L_s} \end{bmatrix} \begin{bmatrix} i_a \\ i_b \\ i_c \end{bmatrix} + \frac{1}{L_s}\begin{bmatrix} V_{s_a} - V_{i_a} \\ V_{s_b} - V_{i_b} \\ V_{s_c} - V_{i_c} \end{bmatrix}. \tag{3}$$

Here, V_{sabc} is AC grid voltage, V_{iabc} is inverter output voltage, i_{sabc} is AC output currents of the inverter, L_s is coupling inductance, and R_s is internal resistance of coupling inductance. Three-phase systems are conventionally modeled and controlled in the *dq*-coordinate system. This transformation has advantages such as mapping onto two variables three variables of the original coordinates and independent control of active and reactive components by using these variables [38]. Therefore, the circuit equation of the D-STATCOM's AC side in *abc* coordinates is converted to *dq*-axis coordinates. For this aim, both sides of Eq. (3) are multiplied by transformation matrix K given in Eq. (4):

$$K = \frac{2}{3}\begin{bmatrix} \cos\omega t & \cos(\omega t - 120^\circ) & \cos(\omega t + 120^\circ) \\ \sin\omega t & \sin(\omega t - 120^\circ) & \sin(\omega t + 120^\circ) \\ \frac{1}{\sqrt{2}} & \frac{1}{\sqrt{2}} & \frac{1}{\sqrt{2}} \end{bmatrix}. \tag{4}$$

Here, ω is angular frequency of the AC grid. Circuit equations of the D-STATCOM in *dq*-axis coordinates are obtained as follows [38]:

$$\frac{di_d}{dt} = -\frac{R_s}{L_s}i_d + \omega i_q + \frac{1}{L_s}(V_{s_d} - V_{i_d}), \tag{5}$$

$$\frac{di_q}{dt} = -\frac{R_s}{L_s}i_q - \omega i_d + \frac{1}{L_s}(V_{s_q} - V_{i_q}). \tag{6}$$

Here, V_{sd} and V_{sq} are *dq*-axis components of AC grid voltage, V_{id} and V_{iq} are *dq*-axis components of inverter voltage, and i_d and i_q are *dq*-axis currents of the inverter. V_{id} and V_{iq} are also defined by Eq. (7):

$$\begin{aligned} V_{i_d} &= M_a V_{D_C}\cos\delta, \\ V_{i_q} &= M_a V_{D_C}\sin\delta. \end{aligned} \tag{7}$$

In Eq. (7), M_a is the modulation index and V_{DC} is the DC-link voltage of the inverter. The DC-link current in the *dq*-axis is expressed as follows:

$$i_{d_c} = M_a V_{DC}\cos\delta = \frac{3}{2}M_a(i_d\cos\delta - i_q\sin\delta). \tag{8}$$

The DC-side dynamic model of the D-STATCOM in the dq-axis is obtained by using Eq. (8) as follows:

$$\frac{dV_{DC}}{dt} = M_a V_{DC}\cos\delta = \frac{3M_a}{2C}(i_d\cos\delta - i_q s \in \delta). \tag{9}$$

The AC side dynamic model of the D-STATCOM in the *dq*-axis is presented by Eq. (5) and Eq. (6) and the DC side dynamic model of the D-STATCOM in the *dq*-axis is presented by Eq. (9).

3. Structure of neuro-fuzzy controller

The FLC is able to make inferences from expert knowledge and the ANN has feature abilities such as learning, generalization, and adaptation. The NFC is an intelligent control method combining features of the FLC and ANN. Basically, the NFC is based on the principle implemented by ANN for the functions of the FLC [39]. Therefore, NFCs show features of a nonlinear controller that has abilities such as learning, adaptation, and ability to make inferences. In addition, NFCs do not need a mathematical model of the system to be controlled. These features make NFCs superior when compared with other conventional controllers.

In this study, an NFC with two inputs and one output is used for the control of the D-STATCOM's dq-axis currents. Error of the d-axis current and change in error are given as inputs to the NFC used for control of the d-axis current. The q-axis current is controlled by an NFC in a manner similar to the control of the d-axis current. For an NFC with singleton rules, a common rule set with two fuzzy if-then is given as follows [40]:

$$R^j: \; IF \; X_1 \; is \; A_1^j, \;\; X_2 \;\; is \;\; A_2^j, \;\; THEN \; y \; is \; \omega_j. \tag{10}$$

Here, X_1 and X_2 are input variables, y is the output variable, and there are linguistic terms of the precondition part with membership functions and ω_j is a real number of the consequent part. The structure of the neuro-fuzzy network used in this study is shown in Figure 2. Inputs of NFCs used in dq-axis current control are chosen as the error of d- and q-axis current and change of these errors, as given Eqs. (11) and (12):

$$e(k) = i_{d_q}^*(k) - i_{d_q}(k), \tag{11}$$

$$\triangle e(k) = e(k) - \triangle(k-1). \tag{12}$$

Here, e is current tracking error, Δe is changing of the current tracking error, and i_{dq}^* is the reference currents for the d- and q-axis, respectively.

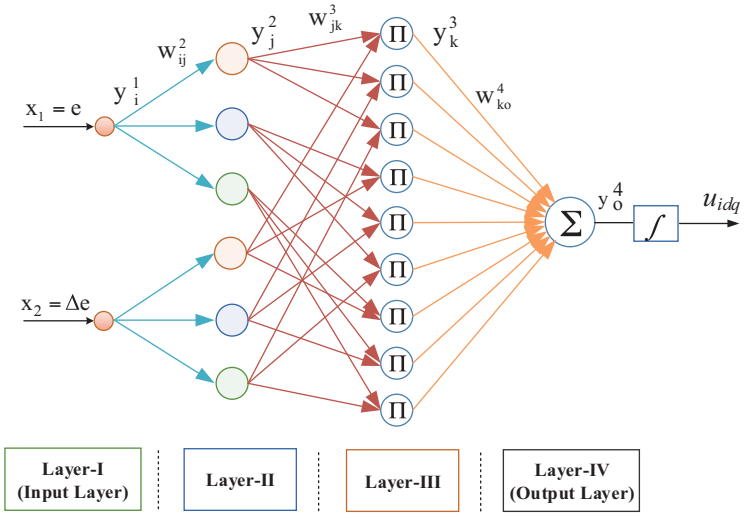

Figure 2. Neuro-fuzzy architecture with singleton rules.

Functions of each layer of the NFC given in Figure 2 are briefly described below [41].

- Layer-I bypasses input signals to the next layer, i.e. $y_i^1 = net_i^1$,
  where net_i^I is the ith input to the node of Layer-I, which includes current error $X_1 = e$ and the change of the error $X_1 = \Delta e$.

- Layer-II calculates the degree of membership functions for the input values. A Gaussian function is utilized to represent the membership functions. The weights between the input and membership layer are assumed to be unity. The output of this layer is expressed as:

$$net_j^2 = -\frac{(X_i - m_{i_j}^2)}{(\sigma_{i_j}^2)}, \tag{13}$$

$$y_j^2 = exp(net_j^2), \tag{14}$$

where σ_{ij} and m_{ij} are the standard deviation and mean of the Gaussian function in the jth term of the ith input node.

- Layer-III of the NFC includes the fuzzy rule base. Each node takes two inputs, one from the membership value for the current error and the other from the membership value for the change in current error. For the kth rule node:

$$net_k^3 = \prod_j \; w_{j_k}^3 \; x_j^3, \tag{15}$$

$$y_k^3 = net_k^3, \tag{16}$$

where X_j^3 represents the jth input to the node of the rule layer and w_{jk}^3 is assumed as unity.

- Layer-IV consists of a single node and collects all incoming signals from the rule layer to obtain the results:

$$net_o^4 = \sum_k \; w_{k_o}^4 \;\; y_k^3. \tag{17}$$

Here, the link weights w_{ko}^4 represent the output action of the kth rule. The output of the system using central defuzzification for the Mamdani fuzzy model is given as [39]:

$$y_o^4 = \frac{net_o^4}{\sum_k y_k^3}. \tag{18}$$

Steady-state error in the output of the NFC is eliminated by using an external integrator. Thus, the desired inverter dq-axis voltages are obtained from integrated outputs of current controllers. The NFC can adjust the fuzzy control rules by modifying the output weights. The parameters of the membership functions and the output weights of the NFC are modified using the backpropagation algorithm to minimize the performance index E:

$$E = \frac{1}{2}e^2. \tag{19}$$

The w_{ko}^4 parameter in Eq. (17) can be modified as follows:

$$w_{ko} = w_{ko} - \gamma \frac{\partial E}{\partial w_{ko}}, \tag{20}$$

where γ is the learning rate. The gradient of performance index E can be derived as follows:

$$\frac{\partial E}{\partial w_{ko}} = -sign(\frac{\partial i_{dq}}{\partial y_o^4}) \frac{\partial y_o^4}{\partial net_o^4} \frac{\partial net_o^4}{\partial w_{k_o}} = \beta \frac{y_k^3}{\sum_k y_k^3}, \tag{21}$$

where $\frac{\partial i_{dq}}{\partial y_o^4}$ should be calculated using the D-STATCOM dynamics. The gradient of performance index E for the parameters of membership functions can be written as follows:

$$\frac{\partial E}{\partial m_{ij}} = -e.sign(\frac{\partial i_{dq}}{\partial y_o^4}) \frac{1}{\sum_k y_k^3} w_{ko}^4 \frac{X_i - m_{ij}}{(\sigma_{ij})^2} y_j^2, \tag{22}$$

$$\frac{\partial E}{\partial \sigma_{ij}} = -e.sign(\frac{\partial i_{dq}}{\partial y_o^4}) \frac{1}{\sum_k y_k^3} w_{ko}^4 \frac{(X_i - m_{ij})^2}{(\sigma_{ij})^3} y_j^2. \tag{23}$$

4. The proposed control structure for the D-STATCOM

Different control algorithms such as phase angle control, constant DC-link schema, and direct and indirect current control methods have been proposed for reactive power control of D-STATCOMs [37]. The indirect current control method has advantages such as using the fixed switching frequency, realizing the complete reactive power compensation, independent control of active and reactive power, and incorporating the self-supporting DC-link [42]. Therefore, an indirect current control method is preferred in this study.

A complete block diagram of the control unit is shown in Figure 3. In this figure, a three-phase software phase locked loop (SPLL) is used to synchronize inverter voltage with the grid voltage. The *abc/dq0* transform block converts three-phase currents to the reference synchronous rotating frame. DC-link voltage is controlled with a conventional PI controller because of the slow dynamics of the DC side. In DC voltage control, the average value of three DC-link capacitor voltages is used. This average DC voltage value is compared with the reference DC voltage value. The DC voltage error obtained is fed to the PI controller. The reference value for d-axis current is obtained from the output of this controller. For changing the AC grid voltage or reactive loads, a setpoint for q-axis current is set by the user as a step command. Therefore, there is no need for an AC voltage/reactive power controller.

The NFC regulates the d- and q-axis currents. Error and change in the error are used as inputs to the NFCs. An anti-wind-up integrator is utilized in the outputs of NFCs to limit the output of the controller and compensate for steady-state error. The integrated outputs of current controllers represent reference values for d- and q-axis components of inverter voltage V_{id} and V_{iq}. The phase angle and modulation index are calculated from these terms and then three-phase modulation signals are produced by using phase angle and the modulation index.

5. Experimental results

The experimental setup of the D-STATCOM is shown in Figure 4. The experimental setup consists of four main parts: the power circuit, DS1103 controller card, measurement and protection circuits, and gate drive

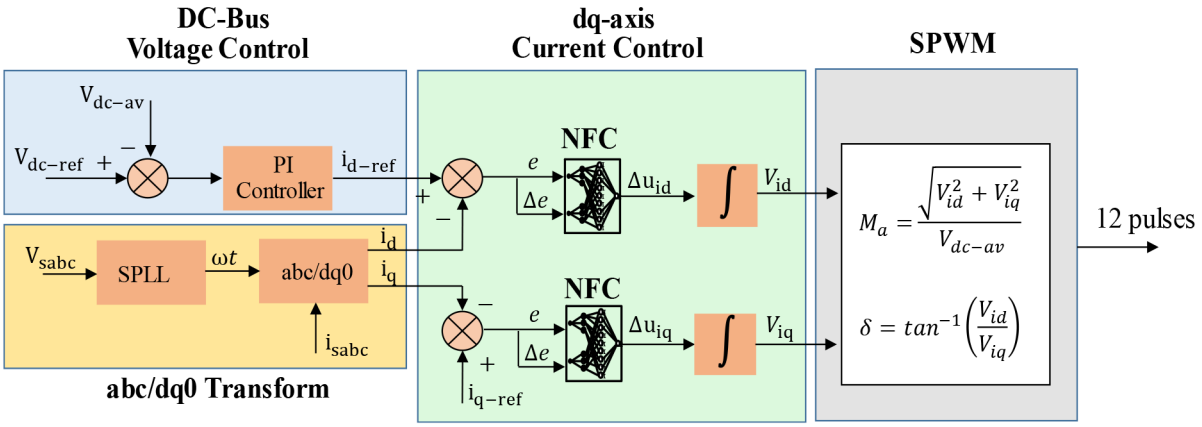

Figure 3. Complete block diagram of NFC current-controlled D-STATCOM.

circuits. In the D-STATCOM power circuit, three IGBT intelligent power modules (IPM-PM75CLA120) are used for the three-level H-bridge inverter. This inverter is connected to the AC grid by a three-phase coupling inductance with internal resistance. PWM signals for the inverter are produced by multilevel SPWM technique with 1.25 kHz switching frequency. For this aim, currents and voltages are sensed by using Hall effect LA50-S/SP1 current and LV25-1000 voltage transducers, respectively. The dSPACE DS1103 controller card is used for real-time control of the D-STATCOM. This controller card includes a PPC750GX/1GHz main processor and Texas Instruments TMS320F240/20MHz slave processor. The DS1103 controller card allows the user to construct the control algorithm in MATLAB/Simulink and then convert the model files to real-time codes using the Real-Time Workshop of MATLAB and Real-Time Interface of dSPACE. The NFC is trained using the simulation model, which is verified by the experimental data obtained from the D-STATCOM, and then the trained NFC is used in experimental study. Real-time values of the physical system variables can be assigned to the user-defined variables using the dSPACE ControlDesk Developer software. In addition, the graphical user interface can be designed by the user to observe the real-time values of the variables or to change the input variables such as reactive current setpoint. Before start-up of the D-STATCOM, the AC grid voltage is adjusted to 200 V by means of an autotransformer to charge the DC-link capacitors. In addition, precharge resistances in series with the DC-link capacitors are connected to limit the initial charging current and then these resistances are bypassed after initial charging of the DC-link capacitor. The parameters of the power circuit are listed in the Table. Detailed information regarding selection of the capacitor and inductor can be founded in [43]. Dynamic compensation performance of the NFC current-controlled D-STATCOM is evaluated for different setpoints of i_{qref}. First, the reactive current setpoint for i_{qref} is changed from standby mode to inductive mode (0 A to –20 A) in the dSPACE ControlDesk environment. This case is presented as Mode-1 in the experimental results.

Then it is changed from standby operation mode to capacitive operation mode (0 A to 20 A). This mode is depicted as Mode-2 in the experimental results. Three DC-link capacitor voltages, phase angle, q-axis current, and AC side current-voltage for different operation conditions mentioned above are depicted in Figure 5. As shown in Figure 5, DC-link capacitor voltages track the setpoint under two operation conditions. In addition, it is seen in Figure 5 that fluctuations in DC-link voltage are higher in capacitive mode. This is due to the longer turn-on duration of inverter switches in capacitive mode than inductive mode. Thus, much more second current

Figure 4. Experimental setup of the D-STATCOM.

Table. Parameters related to experimental setup.

Generated/absorbed reactive power	8.5 kVAR
AC grid voltage/frequency	200 V/50 Hz
Reference DC-link voltage	340.8 V
Coupling inductance	2.89 mH
Internal resistance of coupling inductance	0.1 ohm
DC-link capacitors	3.3 mF/450 V
Switching frequency	1.25 kHz
Sampling time	100 μ s

harmonic is drawn from the DC-link capacitors. The phase angle is a lower value in capacitive operation mode when compared with inductive operation mode so that active power flowing to the inverter remains constant. The reactive current quickly tracks its setpoint without overshooting in both operating modes. Furthermore, the inverter operates with a lower modulation index M_a in inductive operation mode compared with standby operation mode, whereas there is a higher modulation index M_a in capacitive operation mode compared with standby operation mode. In addition, there is no steady-state error in DC-link voltages and reactive current components for each operation mode.

The performance of the D-STATCOM with NFC current controlled is also evaluated for transition from inductive operation mode to capacitive operation mode and vice versa. For these operation modes, the reference reactive current command is changed from –20 A to 20 A. This operation mode is presented as Mode-3. In addition, the reactive current setpoint is changed from 20 A to –20 A. This operation mode is Mode-4. The experimental results obtained from these operation conditions are depicted in Figure 6. It is seen that DC-link voltages are balanced and they are held at the reference value. These figures show that the reactive current is at its reference value in spite of the worst operating conditions (inductive operation mode to capacitive operation mode and vice versa). Since the DC-link voltage is constant in the indirect current control technique, reactive power exchange between the D-STATCOM and AC grid is carried out by changing modulation index M_a. Compared with standby mode, M_a has a lower value in inductive operation mode and a higher value in capacitive operation mode. It is seen that the D-STATCOM operates with a higher modulation index in capacitive operation mode to increase the amplitude of the inverter output voltage. In addition, there is no DC voltage error and reactive current error in steady state in both operating modes. Investigating the AC side voltage and current for phase-a, there is no current flowing until the reference reactive current command is changed to –20 A (at approximately 0.615 s). The AC side current of the D-STATCOM is lagging by about

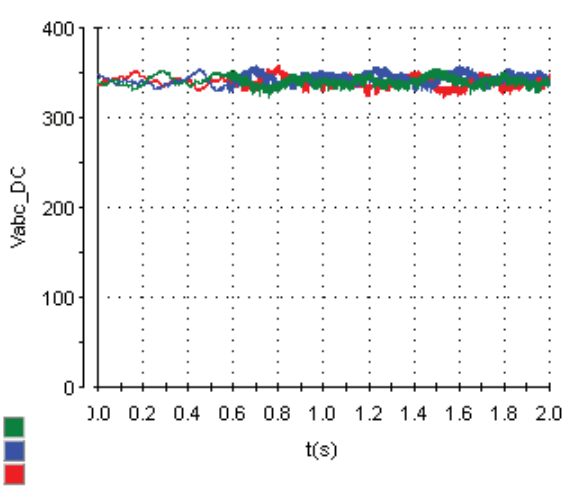

(a) DC-link voltages in Mode-1

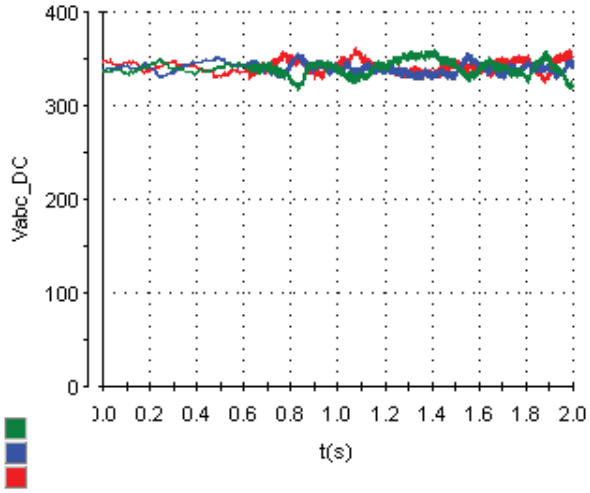

(b) DC-link voltages in Mode-2

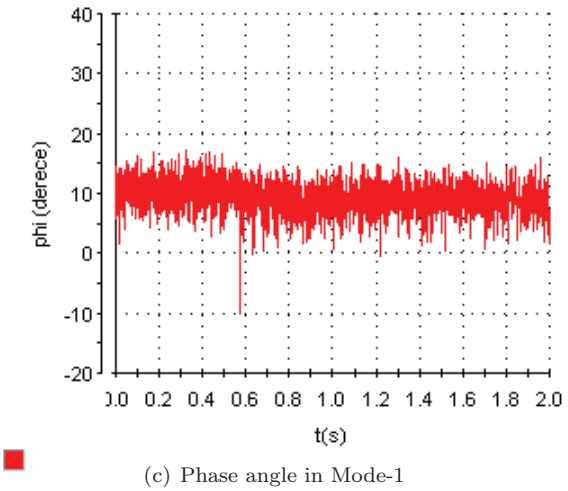

(c) Phase angle in Mode-1

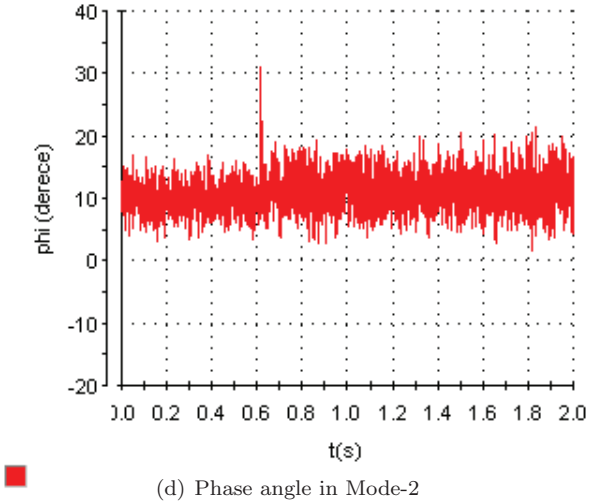

(d) Phase angle in Mode-2

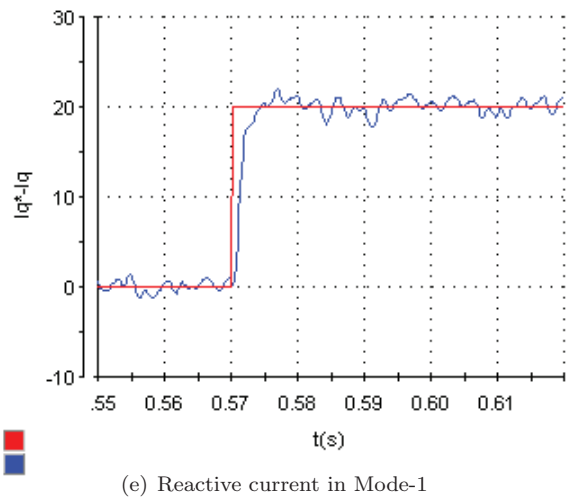

(e) Reactive current in Mode-1

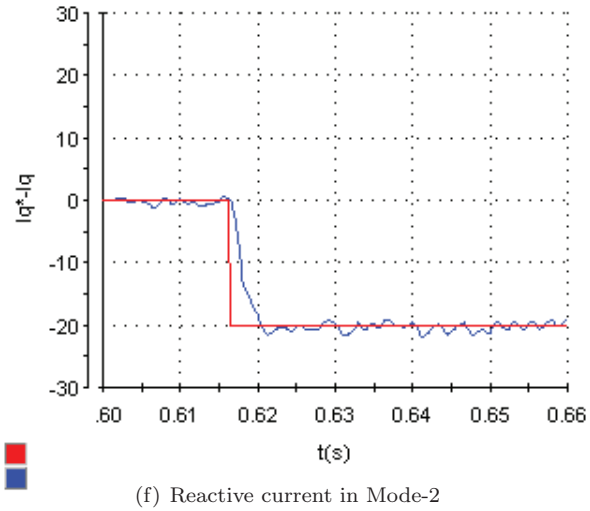

(f) Reactive current in Mode-2

Figure 5. Experimental results for Mode-1 and Mode-2 operations.

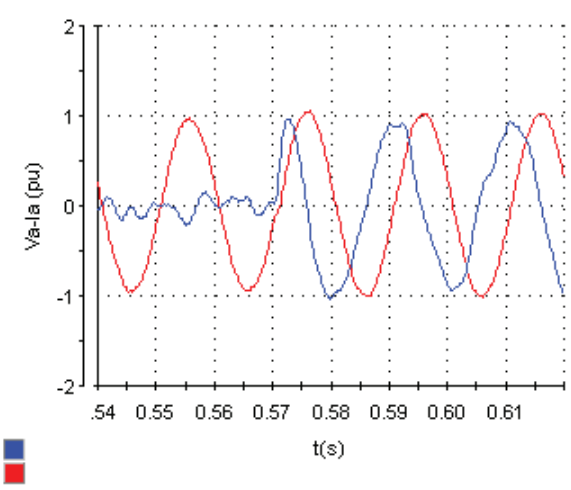

(g) Voltage and current in Mode-1

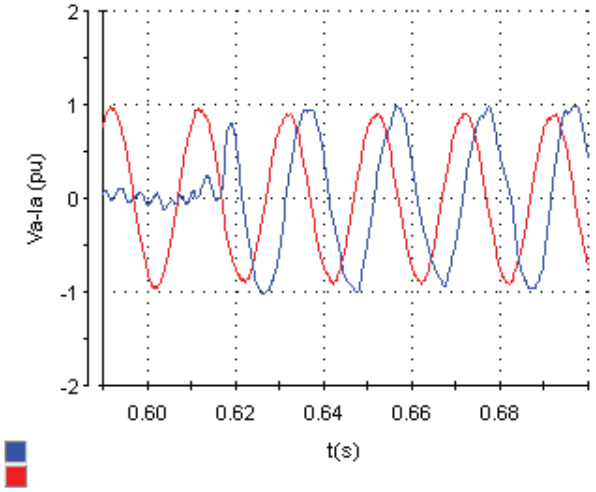

(h) Voltage and current in Mode-2

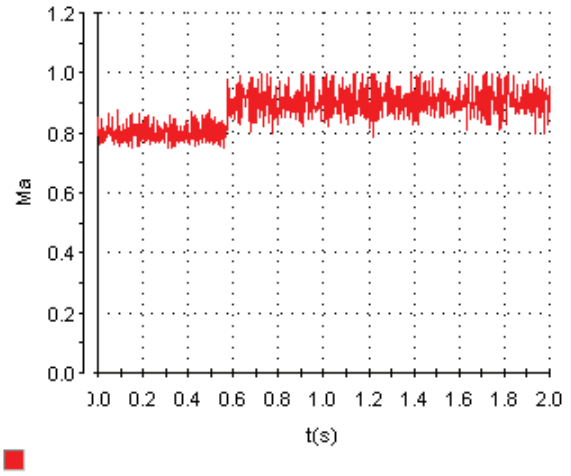

(i) Modulation index in Mode-1

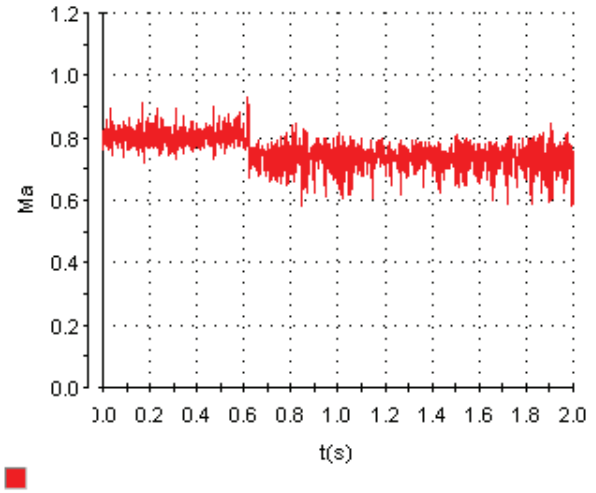

(j) Modulation index in Mode-2

Figure 5. Continued.

90° with respect to its voltage for inductive operation mode and after the reference reactive current command is changed from –20 A to 20 A the AC side current of the D-STATCOM is leading by about 90° with respect to its voltage.

6. Conclusion

In this paper, a D-STATCOM's *dq*-axis current is controlled by using an NFC. The performance of the NFC current-controlled D-STATCOM is evaluated for different operation modes. Operation modes are considered as standby mode to inductive operation mode, standby mode to capacitive operation mode, inductive operation mode to capacitive operation mode, and capacitive operation mode to inductive operation mode. Responses of the D-STATCOM's reactive current and DC-link voltages are investigated under these operation conditions. The NFC current-controlled D-STATCOM provides good dynamic response and tracking ability under all operation conditions. Experimental results show that the NFC current-controlled D-STATCOM can provide the desired exact and fast reactive power within its own rated power limits even in the worst operation conditions.

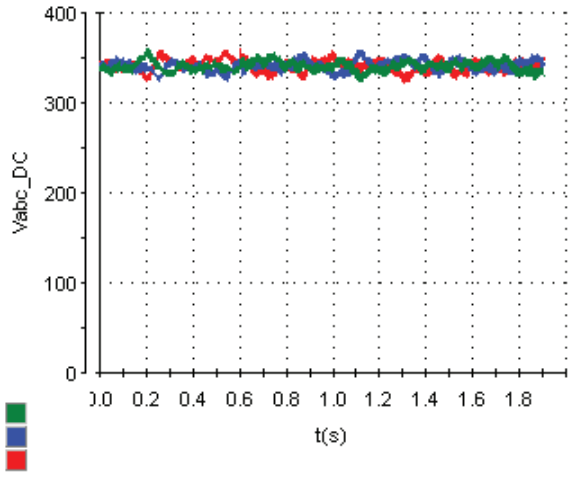

(a) DC-link voltages in Mode-3

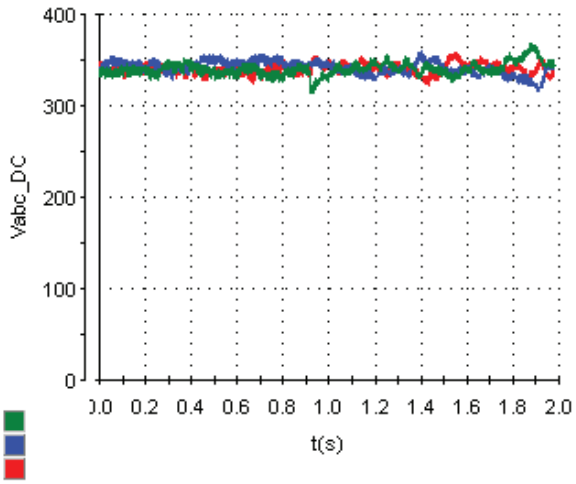

(b) DC-link voltages in Mode-4

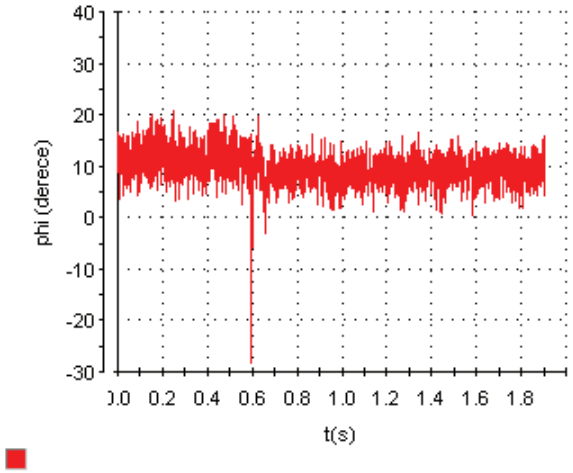

(c) Phase angle in Mode-3

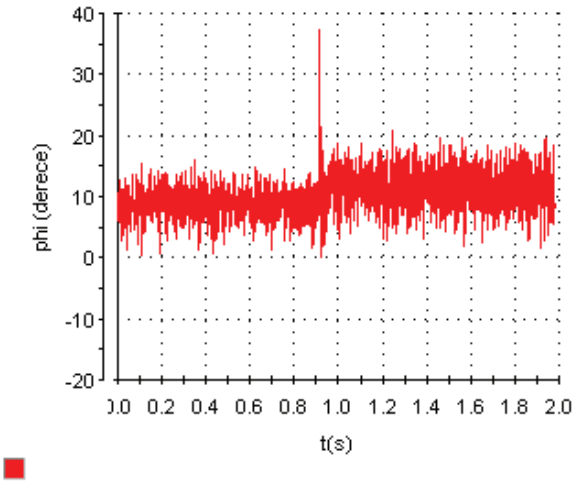

(d) Phase angle in Mode-4

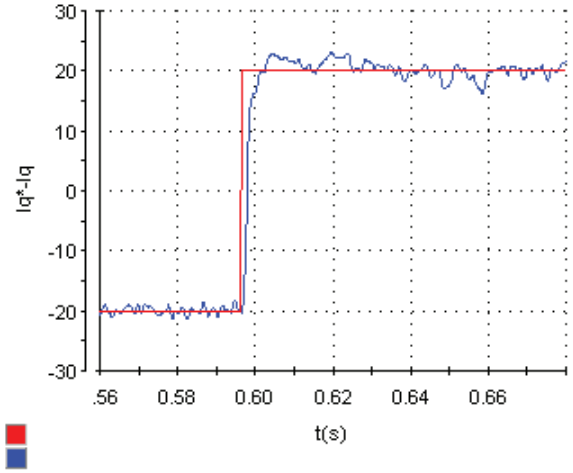

(e) Reactive current in Mode-3

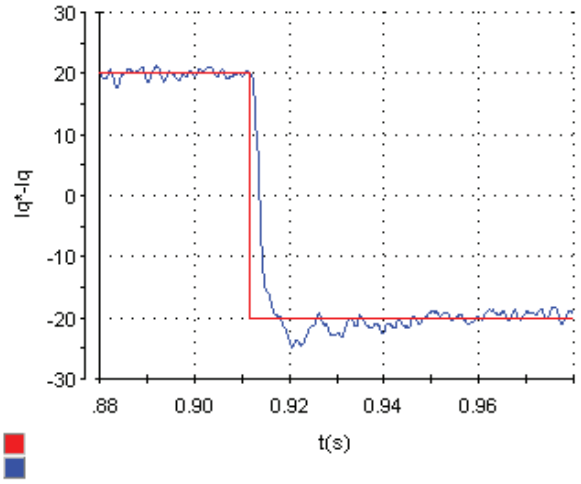

(f) Reactive current in Mode-4

Figure 6. Experimental results for Mode-3 and Mode-4 operations.

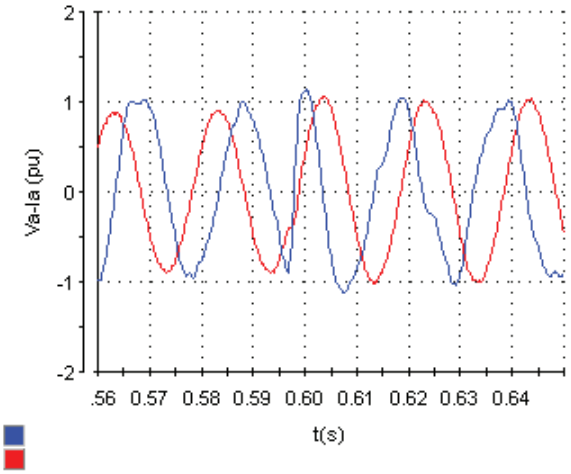

(g) Voltage and current in Mode-3

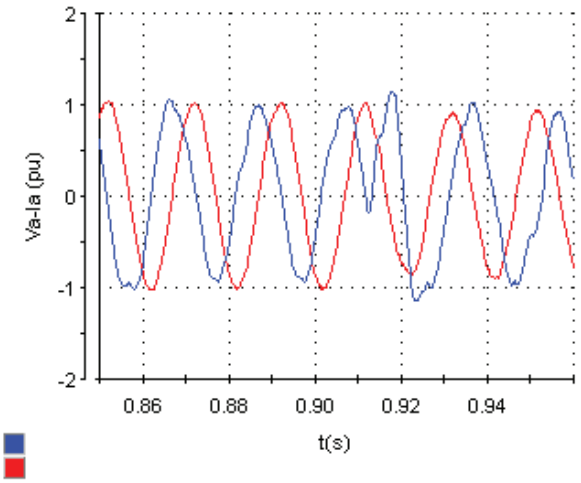

(h) Voltage and current in Mode-4

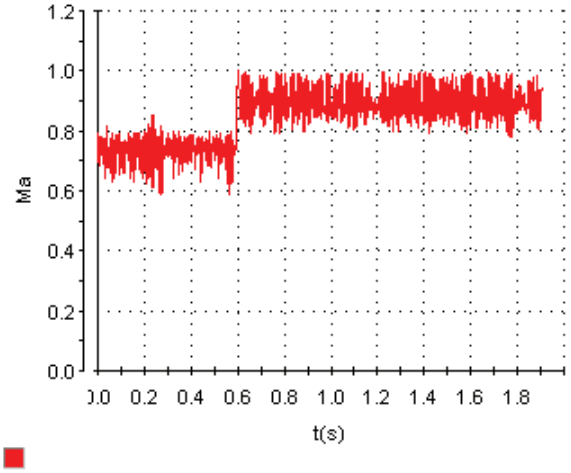

(i) Modulation index in Mode-3

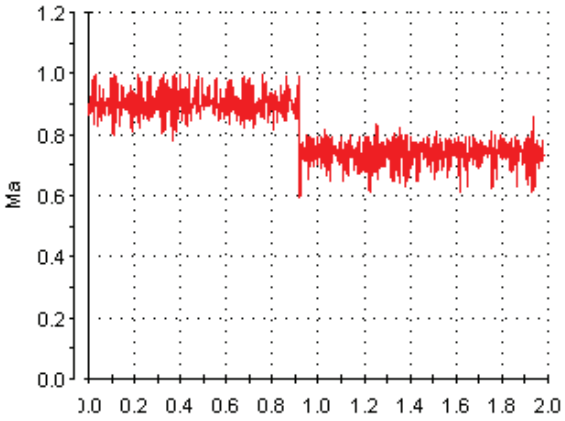

(j) Modulation index in Mode-4

Figure 6. Continued.

Acknowledgment

This work was supported by the Scientific and Technological Research Council of Turkey (TÜBİTAK) with project number 107E245, titled "Implementation of Three-Level H-bridge Inverter Based Distribution Static Synchronous Compensator for Dynamic Compensation in Distribution Systems".

References

[1] Singh B, Solanki J. An improved control approach for DSTATCOM with distorted and unbalanced AC mains. J Power Electron 2008; 8: 131-140.

[2] Mahdianpoor M, Kiyoumarsi A, Ataei M, Hooshmand RA, Karimi H. A multifunctional DSTATCOM for power quality improvement. Turk J Electr Eng Co 2017; 25: 172-183.

[3] Ahmad MT, Kumar N, Singh B. Generalised neural network-based control algorithm for DSTATCOM in distribution systems. IET Power Electron 2017; 10: 1529-1538.

[4] Singh B, Saha R, Chandra A, Al-Haddad K. Static synchronous compensators (STATCOM): a review. IET Power Electron 2008; 2: 297-324.

[5] Yang X, Zhong Y, Wang Y. A novel control method for DSTATCOM using artificial neural network. In: Fifth International Power Electronics and Motion Control Conference; 14–16 August 2006; Shanghai, China. New York, NY, USA: IEEE. pp. 1-4.

[6] Schauder C, Mehta H. Vector analysis and control of advanced static VAr compensators, Generation. IEE Proc-C 1993; 140: 299-360.

[7] Blasko V, Kaura V. A New mathematical model and control of a three-phase AC-DC voltage source converter. IEEE Power Electr 1997; 12: 116-123.

[8] Adzic ME, Grabic SU, Katic VA. Analysis, control and design of STATCOM in distribution network voltage control mode. In: Sixth Nikola Tesla International Symposium; 18–20 October 2006; Belgrade, Serbia. pp. 1-4.

[9] Suul JA, Molinas M, Norum L, Undeland T. Tuning of control loops for grid connected voltage source converters. In: 2nd IEEE International Conference on Power and Energy; 1–3 December 2008; Johor Bahru, Malaysia. New York, NY, USA: IEEE. pp. 792-802.

[10] Sirisukprasert S, Huang AQ, Lai JS. Modeling, analysis and control of cascaded- multilevel converter-based STATCOM. In: IEEE 2008 Power Engineering Society General Meeting; 13–17 July 2003; Toronto, Canada. New York, NY, USA: IEEE. pp. 2561-2568.

[11] Gui Y, Lee YO, Youngseong H, Kim W, Chung CC. Passivity-based control with nonlinear damping for STATCOM system. In: IEEE Conference on Decision and Control; 10–13 December 2012; Maui, HI, USA. New York, NY, USA: IEEE. pp. 1715-1720.

[12] Petitclair P, Bacha S, Ferrieux JP. Optimized linearization via feedback control law for a STATCOM. In: 32nd Industry Applications Conference; 5–9 October 1997; New Orleans, LA, USA. New York, NY, USA: IEEE. pp. 880-885.

[13] Petitclair P, Bacha S, Rognon JP. Averaged modelling and nonlinear control of an advanced static VAr compensator. In: IEEE 1996 Power Electronics Specialists Conference; 23–27 June 1996; Baveno, Italy. New York, NY, USA: IEEE. pp. 753-758.

[14] Han Y, Lee OY, Chung CC. A modified nonlinear damping of zero-dynamics via feedback control for a STATCOM. In: IEEE PowerTech Conference; 28 June–2 July 2009; Bucharest, Romania. New York, NY, USA: IEEE. pp. 880-885.

[15] Kanchanaharuthai A, Chankong V, Loparo K. Transient stability and voltage regulation in power systems with renewable distributed energy resources. In: Energytech; 25–26 May 2011; Cleveland, OH, USA. New York, NY, USA: IEEE. pp. 1-6.

[16] Liu F, Mei S, Lu Q, Ni Y, Wu FF, Yokoyama A. The nonlinear internal control of STATCOM: theory and application. Int J Elec Power 2003; 25: 421-430.

[17] Yao Z, Kesimpar P, Donescu V, Uchevin N, Rajagopalan V. Nonlinear control for STATCOM based on differential algebra. In: IEEE 1998 Power Electronics Specialists Conference; 22–22 May 1998; Fukuoka, Japan. New York, NY, USA: IEEE. pp. 329-334.

[18] Bouafia S, Benaissa A, Barkat S, Bouzidi M. Second order sliding mode control of three-level four-leg DSTATCOM based on instantaneous symmetrical components theory. Energy Syst 2016; 1: 1-33.

[19] Bouafia S, Benaissa A, Barkat S. Integral sliding mode control of four-leg DSTATCOM coupled with SMES unit. In: 5th International Conference on Electrical Engineering; 29–31 October 2017; Boumerdes, Algeria. New York, NY, USA: IEEE. pp. 1-6.

[20] Singh B, Sabha RA. Adaptive theory-based improved linear sinusoidal tracer control algorithm for DSTATCOM. IEEE Power Electr 2013; 28: 3768-3778.

[21] Gokbulut M, Dandil B, Bal C. A hybrid neuro-fuzzy controller for brushless DC motors. Lect Notes Comp Sci 2006; 3949: 125-132.

[22] Jayachandran J, Sachithanandam RM. Neural network-based control algorithm for DSTATCOM under nonideal source voltage and varying load conditions. Can J Elect Comput E 2015; 38: 307-317.

[23] Mohaddes M, Gole AM, McLaren PG. A neural network controlled optimal pulse-width modulated STATCOM. IEEE T Power Deliver 1999; 14: 481-488.

[24] Ahmad MT, Narendra K, Bhim S. Generalised neural network-based control algorithm for DSTATCOM in distribution systems. IET Power Electron 2017; 10: 1529-1538.

[25] Suryanarayana H, Mahesh KM. Fuzzy logic based supervision of dc link PI control in a DSTATCOM. In: India Conference 2008; 11–13 December 2008; Kanpur, India. New York, NY, USA: IEEE. pp. 1-6.

[26] Valderrábano A, Juan MR. DSTATCOM regulation by a fuzzy segmented PI controller. Electr Pow Syst Res 2010; 80: 707-715.

[27] Coteli R, Dandil B, Ata F. Fuzzy-PI current controlled D-STATCOM. Gazi University Journal of Science 2011; 24: 91-99.

[28] Coteli R, Acikgoz H, Ucar F, Dandil B. Design and implementation of type-2 fuzzy neural system controller for PWM rectifiers. Int J Hydrogen Energ 2017; 42: 20759-20771.

[29] Mohagheghi S, Venayagamoorthy GK, Harley RG. Optimal neuro-fuzzy external controller for a STATCOM in the 12-bus benchmark power system. IEEE Power Deliver 2007; 22: 2548-2558.

[30] Mohagheghi S, Venayagamoorthy GK, Harley RG. Adaptive critic design based neuro-fuzzy controller for a static compensator in a multimachine power system. IEEE Power Syst 2006; 21: 1744-1754.

[31] Mohr M, Fuchs FW. Comparison of three phase current source inverters and voltage source inverters linked with DC to DC boost converters for fuel cell generation systems. In: IEEE 2005 Power Electronics and Applications; 11–14 September 2005; Dresden, Germany. New York, NY, USA: IEEE. pp. 1-10.

[32] El-Moursi MS, Sharaf AM. Novel reactive power controllers for the STATCOM and SSSC. Electr Pow Syst Res 2006; 76: 228-241.

[33] Gonzalez PB, Cerrada AG. Control system for a PWM-based STATCOM. IEEE Power Delivery 2000; 15: 1252-1257.

[34] Choi NS, Cho JG, Cho GH. A general circuit topology of multilevel inverter. In: IEEE 1991 Power Electronics Specialists Conference; 24–27 June 1991; Cambridge, MA, USA. New York, NY, USA: IEEE. pp. 96-103.

[35] Anadol MA, Aydın M, Yalçınöz T. A real-time extraction of active and reactive current using microcontrollers for a multipulse STATCOM. Turk J Electr Eng Co 2013; 21: 1044-1060.

[36] Tuncer S, Dandil B. Adaptive neuro-fuzzy current control for multilevel inverter fed induction motor. COMPEL 2008; 27: 668-681.

[37] Çetin A. Design and implementation of a voltage source converter based STATCOM for reactive power compensation and harmonic filtering. PhD, Middle East Technical University, Ankara, Turkey, 2007.

[38] Saeedifard M. Space vector modulation of multilevel and multi-module converters for high power applications. PhD, University of Toronto, Toronto, Canada, 2008.

[39] Jang JSR, Sun CT, Mizutani E. Neuro-Fuzzy and Soft Computing. Upper Saddle River, NJ, USA: Prentice Hall, 1997.

[40] Dandil B. Fuzzy neural network IP controller for robust position control of induction motor drive. Expert Syst Appl 2009; 36: 4528-4534.

[41] Gokbulut M, Dandil B, Bal C. Development and implementation of a fuzzy-neural network controller for brushless DC drives. Intell Autom Soft Co 2007; 13: 415-427.

[42] Masand D, Shailendra J, Gayatri A. Control strategies for distribution static compensator for power quality improvement. IETE J Res 2008; 54: 421-428.

[43] Deniz E, Çöteli R, Dandıl B, Tuncer S. Design and implementation of three level H-bridge inverter based D-STATCOM. Journal of the Faculty of Engineering and Architecture of Gazi University 2011; 26: 289-298.